Tsvetkov, Zh. Eksp. Teor. Fiz. **70**, 1501 (1976) [Sov. Phys. JETP **43**, 783 (1976)].
[2]Ya. E. Pokrovskiĭ and K. I. Svistunova, Fiz. Tekh. Poluprovodn. **4**, 491 (1970) [Sov. Phys. Semicond. **4**, 409 (1970].
[3]J. P. Wolfe, W. L. Hansen, E. E. Haller, R. S. Markiewicz, C. Kittel, and C. D. Jeffries, Phys. Rev. Lett. **34**, 1292 (1975).
[4]Ya. Pokrovskii, Phys. Status Solidi **11**, 385 (1972).
[5]V. G. Lysenko, V. I. Revenko, T. G. Tratas, and V. B. Timofeev, Zh. Eksp. Teor. Fiz. **68**, 335 (1975) [Sov. Phys. JETP **41**, 163 (1975)].
[6]V. A. Benderskiĭ, V. Kh. Brikenshteĭn, V. L. Broude, and I. I. Tartakovskiĭ, Pis'ma Zh. Eksp. Teor. Fiz. **22**, 332 (1975) [JETP Lett. **22**, 156 (1975)].
[7]V. A. Benderskiĭ, V. Kh. Brikenshteĭn, V. L. Broude, and A. G. Lavrushko, Pis'ma Zh. Eksp. Teor. Fiz. **17**, 472 (1973) [JETP Lett. **17**, 339 (1973)].
[8]O. S. Avanesjan, V. A. Benderskii, V. Kh. Brikenstein, V. L. Broude, L. I. Korshunov, A. G. Lavrushko, and I. I. Tartakovskii, Mol. Cryst. Liq. Cryst. **29**, 165 (1974).
[9]O. S. Avanesyan, V. A. Benderskiĭ, V. Kh. Brikenshteĭn, V. L. Broude, A. G. Lavrushko, and I. I. Tartakovskii, Kvantovaya Elektron. (Moscow) **4**, No. 4 (1977) [Sov. J. Quantum Electron. **7**, No. 4 (1977)].
[10]V. A. Benderskiĭ, V. Kh. Brikenstein, V. L. Broude, and A. G. Lavrushko, Solid State Commun. **15**, 1235 (1974).
[11]A. V. Bree and L. E. Lyons, J. Chem. Soc. (Lond.) 2262 (1956).
[12]P. Goursot, H. L. Girdnar, and E. F. Westrum, J. Phys. Chem. **74**, 2638 (1970).
[13]A. A. Ovchinnikov, Zh. Eksp. Teor. Fiz. **57**, 2137 (1969) [Sov. Phys. JETP **30**, 1160 (1970)].
[14]V. M. Agranovich, Teoriya eksitonov (Exciton Theory), Nauka, 1968, (a) Ch. 10, (b) Ch. 2, § 9.
[15]T. D. Lee, K. Huang, and C. N. Yang, Phys. Rev. **106**, 1135 (1957).

Translated by J. G. Adashko

Measurement of the electron temperature and density distributions in the plasma in the TM-3 Tokamak installation by the method of laser radiation scattering

V. V. Sannikov

(Submitted February 23, 1976)
Zh. Eksp. Teor. Fiz. **72**, 119–126 (January 1977)

Electron temperatures of 0.15–1.2 keV have been measured at plasma densities $\bar{n}_e = 6\times10^{12}$–$6\times10^{13}$ cm^{-3} under stable discharge conditions in the TM-3 Tokamak installation by the method of Thomson scattering. The electron temperature and density distributions along the plasma column radius have been obtained for different plasma parameters. The variation in time of the plasma-electron density and temperature profiles has been measured in one of the standard regimes ($H_z = 22$kOe, $J = 50$ kA, $\bar{n}_e = 6\times10^{13}$ cm^{-3}). The diamagnetic and laser measurements have been compared.

PACS numbers: 52.55.Gb, 52.70.Kz, 52.25.Lp

1. INTRODUCTION

The application of the technique of laser probing of a plasma in installations of the Tokamak type has allowed the accumulation of a large quantity of information about the local density, n_e, and temperature, T_e, of the electrons in the plasma column.[1–6] Of indubitable interest is the problem of the measurement of the distributions $T_e(r)$ and $n_e(r)$ on the TM-3 Tokamak installation, whose operating conditions allow the variation of the plasma parameters in a wide range of values. However, the small transverse dimensions of the diagnostic port on the installation limit considerably the transmission of the collection optics, and make it impossible for a diaphragm and a trap to be mounted for the purpose of suppressing the parasitic light scattered from the windows and walls of the vacuum chamber. On account of this, the fraction of the parasitic scattered light in the TM-3 facility attains an appreciable value. It becomes necessary to prepare the apparatus for Thomson scattering with appreciable suppression of the parasitic background.

In the experiment we used a polychromator assembled on the basis of the high-transmission MDR-2 diffraction monochromator[7] with a selective ruby filter. The filter, which was 12 mm thick, was cut from a ruby crystal (with a chromium concentration in parts by weight in the blend of 0.5). Absorption in ruby depends on the orientation of the electric vector of the incident radiation relative to the optical axis of the crystal.[8] The filter was mounted in front of the entrance slit of the polychromator in such a way that the optical axis of the crystal was perpendicular to the polarization of the scattered light. Maximum absorption in the ruby line, R_1, is realized in this case. It was possible to reduce the intensity of the $\lambda_0 = 6943$ Å parasitic line, scattered from the windows and walls of the vacuum chamber, by a factor of more than 10^2 with the aid of the selective ruby filter.

The experiment was performed under stable discharge conditions in the Tokamak in the case when the stability safety factor had a value $q > 3$.

2. THE EXPERIMENTAL SETUP

A schematic diagram of the experiment is shown in Fig. 1. Scattered light from a 0.2-cm^3 plasma volume

was collected by an $f/3$ objective at the entrance slit of the polychromator with a 1:1.3 reduction in intensity. The dimensions of the entrance slit were 2×10 mm. Inside the polychromator was mounted a collector consisting of glass light guides that divided the spectrum into five spectral bands each of width 80 Å. In the light-guide unit a light trap was provided for the laser (6943 Å) and the intense H_α spectral (6563 Å) lines. The collector was mounted in such a way that the projection of the entrance slit of the polychromator onto the light guides was on a 1:1 scale. The first channel was centered at 100 Å from the laser line. The polychromator with the selective filter allowed the registration of the scattered-light spectrum corresponding to the electron-temperature range 0.1 to 1.5 keV. The short-wave part of the scattered radiation spectrum was recorded simultaneously on five channels. The signals from the photomultipliers were amplified by preamplifiers (which had a transmission band ~100 MHz and an amplification factor ~15), and were fed to the input sections of S8-2 storage oscillographs. The oscillographs were triggered by a pulse from an FÉK-17 coaxial photocell, which was actuated at the moment of generation by the laser. The laser consisted of a generator with a phototropic shutter and an amplifier. The energy of the radiation was 5 J, the pulse duration at halfwidth was ~50 nsec, and the divergence was ~6 mrad.

The entire receiving channel was calibrated with an S16-40 photometric lamp with a tungsten ribbon filament. The frequency characteristic of the photomultiplier + amplifier system was verified with an AL-102B photodiode, which emitted light pulses of duration 100 nsec in the red region of the spectrum. A special dummy target that could be introduced into the chamber allowed the adjustment of the collection optics along the plasma-column radius in the course of the experiment without destroying the vacuum of the TM-3 installation.

In the Thomson scattering experiment we recorded the relative variation of the electron concentration along the plasma-column radius and during the duration of the discharge. The obtained data were normalized to the readings of a two-millimeter interferometer which recorded the electron density along the diameter of the plasma column. The electron-temperature and concentration distributions were measured on the same side from the plasma center at the points 0.2, 4, and 6 cm.

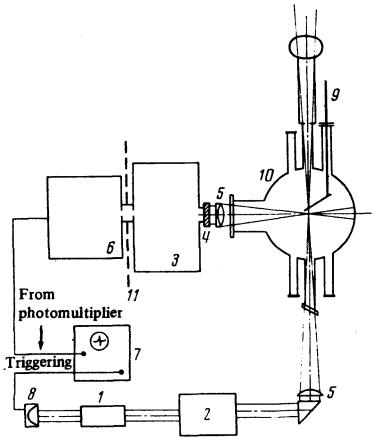

FIG. 1. Schematic diagram of the experimental setup: 1), 2) laser generator and amplifier, 3) polychromator, 4) ruby filter, 5) lenses, 6) photomultiplier unit, 7) oscillograph, 8) FÉK-17 monitor, 9) adjustment dummy target, 10) TM-3 chamber, 11) lead shield.

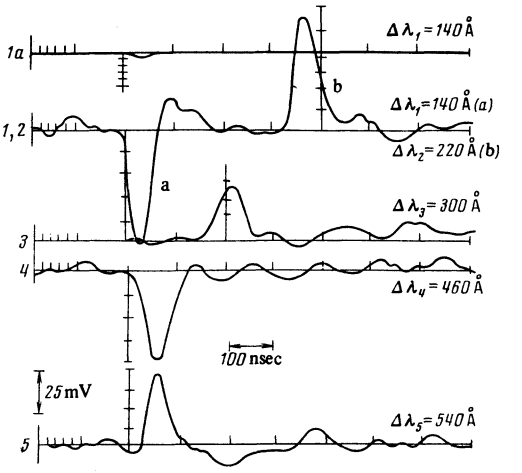

FIG. 2. Oscillograms of the scattered light: 1a) parasitic scattered light signal on the first channel; 1), 2) signals on the first, (a), and second, (b), channels; 3)–5) signals on respectively the third, fourth, and fifth channels.

We used in the experiment RCA-7265 photomultipliers with S-20 photocathodes. Because of the noise fluctuations in the photomultipliers, at low useful-signal levels the experimental results were processed in sets from 5–7 discharges. The amplitude of the parasitic scattered light signal in the first channel is equal to 1–2 mV; the rest of the channels are free of the parasitic background. To protect the photomultipliers from the x rays, we placed a lead shield in front of the photomultiplier unit.

In Fig. 2 we show typical oscillograms of the scattered light. The signal, (b), from the second spectral channel was delayed by a cable for ~300 nsec and fed to one of the entrance sections of the difference amplifier of an oscillograph, to the other entrance section of which was fed the signal, (a), from the first channel. The small amplitude of the signal in the third channel is connected with the lower sensitivity of the photomultiplier of the third channel in comparison with the detectors of the other channels.

The experimental errors range from 10 to 15%, depending on the plasma parameters, and are connected with the fact that the signal amplitude in each of the spectral channels, from which the spectrum of the scattered light is re-established, depends on the quantity $n_e/T_e^{1/2}$, and therefore the accuracy of the measurements depends on the electron density, as well as on the reproducibility of the operating conditions of the installation and the laser.

The experiment was performed at mean—over the diameter—electron concentrations $\bar{n}_e = 6\times10^{12} - 6\times10^{13}$

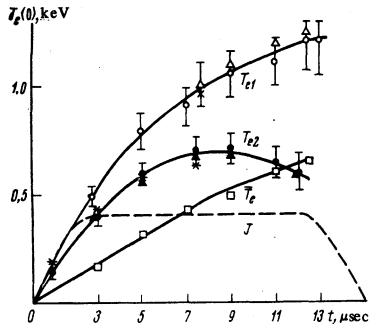

FIG. 3. The variation in time of the electron temperature $T_e(0)$ at the center of the column. For T_{e1} and $\bar{T}_e$ the following regime was maintained: $H_z = 22$ kOe, $J = 49$ kA, the electron concentration in the 7th μsec of the discharge $\bar{n}_e = 6\times10^{13}$ cm^{-3}; for T_{e2}, the regime: $H_z = 22$ kOe, $J = 40$ kA, and $\bar{n}_e = 1.8\times10^{13}$ cm^{-3}. The symbols ○, ●, △, ▲, and X, * on the T_{e1} and T_{e2} curves are experimental points obtained for the corresponding regimes on different days.

cm^{-3}. Electron temperatures T_e in the range 0.15–1.2 keV have been measured.

3. THE EXPERIMENTAL RESULTS

The variation of the electron temperature, $T_e(0)$, at the center of the plasma column during the discharge is shown in Fig. 3. The nature of the heating of the electron component for the regime with a high plasma density and a strong current (the curve T_{e1}) differs from the time dependence with lower current and $\bar{n}_e$ values (the curve T_{e2}): at higher $\bar{n}_e$ values the electron temperature at the center of the column increases toward the end of the discharge to 1.2 keV (with allowance for relativistic corrections),[9,10] whereas at smaller $\bar{n}_e$ values the electron temperature attains its maximum value $T_e(0) = 700$ eV at about 7 μsec into the discharge and has a tendency (within the experimental errors) to decrease toward the end of the discharge. If we estimate the energy lifetime, τ_E, of the central part of the plasma column for these two regimes, then τ_{E1} (the regime corresponding to the electron temperature T_{e1}) is ~10 μsec, while τ_{E2} (the regime with T_{e2}) is ~3 μsec.

It can be assumed that the difference in behavior of

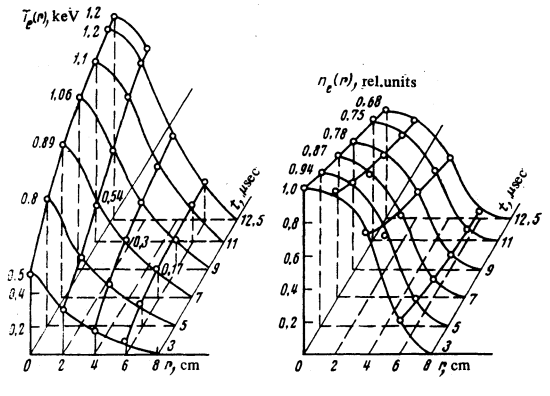

FIG. 4. The variation in time of the plasma-electron temperature and density profiles ($H_z = 22$ kOe, $J = 49$ kA, $\bar{n}_e = 6\times10^{13}$ cm^{-3}).

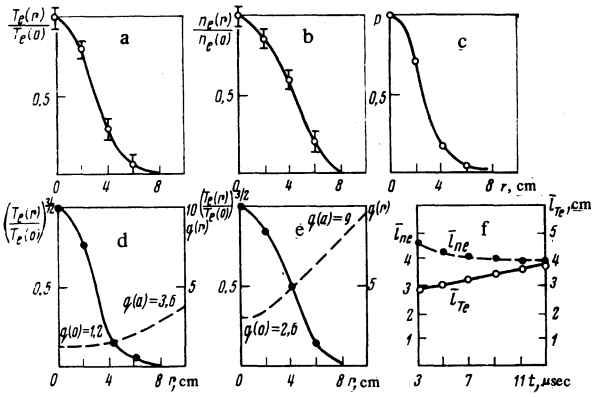

FIG. 5. a) The distribution $T_e(r)$; b) the distribution $n_e(r)$; c) the plasma pressure distribution $P(r)$; d) the current-density and $q(r)$ distributions ($H_z = 22$ kOe, $J = 48$ kA, $\bar{n}_e = 1.4\times10^{13}$ cm^{-3}, $t = 7$ μsec); e) distributions of the current density and the stability safety factor $q(r)$ ($H_z = 21$ kOe, $J = 18.4$ kA, $\bar{n}_e = 6\times10^{12}$ cm^{-3}, $t = 7$ μsec); f) the variation in time of the "temperature radius" l_{Te} and the "density radius" l_{ne} ($H_z = 22$ kOe, $J = 49$ kA, $\bar{n}_e = 6\times10^{13}$ cm^{-3}).

curves T_{e1} and T_{e2} is connected with the fact that in the regime with the lower density the discharge reaches the stationary stage; in the discharge with T_{e1} the stationary stage has not yet been reached.

The difference in behavior of the curves T_{e1} and T_{e2} can also be related with the fact that the temperature profile $T_{e2}(r)$ is flatter than the profile $T_{e1}(r)$, whose variation in the course of the discharge is shown in Fig. 4. The distribution $T_e(r)$ in the regime with T_{e2} was not measured. It is well known that the electron-temperature distribution in a Tokamak installation becomes sharper with increasing plasma density.[2,9] It can be seen from a comparison of Figs. 5d and 5e, which show $(T_e(r)/T_e(0))^{3/2}$ for two regimes differing in the magnitude of the current and the plasma density, that the electron-temperature profile in the TM-3 installation is sharper at a higher $\bar{n}_e$. To verify the reproducibility of the results, we performed a series of check measurements for one and the same regime at different times. In Fig. 3 we also show a typical—for the TM-3—current curve and the time dependence of the mean electron temperature $\bar{T}_e$, computed with the aid of the formula

$$\bar{T}_e = \int_0^a T_e(r)\, n_e(r)\, r\, dr \Big/ \int_0^a n_e(r)\, r\, dr$$

from the profiles measured by means of the laser (Fig. 4). The electron temperature and density distributions along the plasma-column radius for the regime with $\bar{n}_e = 1.4\times10^{13}$ cm^{-3} and $J = 48$ kA are shown in Fig. 5, a) and b). The measurements were carried out in the 7th μsec in the stationary part of the discharge. The plasma-pressure distribution along the column radius (Fig. 5c) was obtained as a product of the functions $T_e(r) + \gamma T_i(r)$ and $n_e(r)$, it being assumed that the distribution $T_i(r)$ coincided with the distribution $T_e(r)$ and that the impurity concentration was small, i.e., $\gamma = n_i/n_e \approx 1$. The ion temperature $T_i(0)$ was computed with the aid of Artsimovich's formula[11]

$$T_i(0)=\frac{6\cdot10^{-7}}{A_i^{1/2}}(JH_z n_e R^2)^{1/2},$$

where A_i is the atomic weight of the substance and R is the great radius of the installation. In the investigated regimes the ion temperature was substantially lower than the electron temperature; therefore, we assumed, for simplicity, that $Z_{eff}\sim 1$, since the existence of $Z_{eff}>1$ (which reduces the number of protons in the discharge) only decreases $\langle n_i T_i\rangle$, leaving virtually unchanged the magnitude of the computed plasma pressure and, consequently, the magnitude of β_J.

The distribution $T_e(r)$ is sharper than $n_e(r)$ in all the investigated regimes. The distribution $n_e(r)$ is close to a parabolic distribution; thus, for example, the density profile in Fig. 5b is close to a parabola of the form

$$n_e(r)=n_e(0)\,[1-(r/a)^2]^2.$$

The obtained distributions $T_e(r)$ and $n_e(r)$ in the TM-3 installation are sharper than those measured earlier on the T-3A installation[1-3]; the sharp electron temperature and density profiles are also typical of other Tokamak installations.[4-6]

Assuming that the current density in the plasma $j(r)\sim T_e^{3/2}(r)$, we computed with the aid of the formula

$$q(r)=2.5H_z r^2/\pi R\int_0 j(r)\,r\,dr,$$

the distribution, $q(r)$, along the column radius, of the safety factor for the plasma stability. The current-density distribution $j(r)\sim[T_e(r)/T_e(0)]^{3/2}$ and the distribution $q(r)$ along the column radius for two different regimes are shown in Fig. 5e. If we introduce the "temperature radius" l_{Te} and the "density radius" l_{ne} defined by

$$l_{Te}=\int_0^a T_e(r)\,dr/T_e(0),\quad l_{ne}=\int_0^a n_e(r)\,dr/n_e(0),$$

then we can estimate from the $T_e(r)$ and $n_e(r)$ profiles shown in Fig. 4 the variation of the hot zone of the plasma during the discharge pulse. The values of l_{Te} and l_{ne} as functions of the time are given in Fig. 5f, from which it can be seen that, toward the end of the discharge, there occurs, along with the growth of the electron temperature at the center of the column, expansion of the hot zone toward the periphery; the density profile $n_e(r)$ does not change significantly during the discharge.

In Fig. 6 we show the dependence of the electron temperature, $T_e(0)$, at the center of the column on the mean electron concentration for a fixed value of the current. As the electron concentration increases, $T_e(0)$, measured by means of the laser, increases. This dependence is at variance with the measurements made on the T-3A,[2] where the electron temperature, measured at the maximum current value of 130 kA, is proportional to $1/n_e(0)$.[2,3] It should be noted that in all the investigated regimes the distributions $T_e(r)$ and $n_e(r)$ in the T-3A installation are very flat, and virtually do not vary with $\bar{n}_e$. The $T_e(r)$ and $n_e(r)$ profiles in the TM-3 installation are substantially sharper than in the T-3A, and become still sharper with increasing electron concentration. As is well known,[13] the energy lifetime of the plasma increases with increasing plasma density. If, as n_e increases, the thermal insulation of the plasma improves, while the distributions $T_e(r)$ and $n_e(r)$ become sharper, then we can attempt to attribute the dependence of $T_e(0)$ on $\bar{n}_e$ in Fig. 6 to the "swooping" of the column as the plasma concentration increases. However, the distributions $T_e(r)$ and $n_e(r)$ were not measured in this case, and therefore the above-indicated proposition requires further careful study.

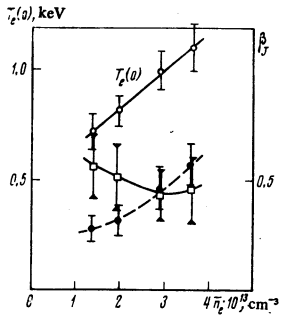

FIG. 6. Dependence on the plasma density of $T_e(0)$ for J = const. Dependence of the laser β_{Jl} (continuous curve) and the diamagnetic β_{Jd} (dashed curve) on the plasma density (H_z = 22 kOe, J = 50 kA, t = 7 μsec).

In Fig. 6 we also present the plots of $\beta_{Jd}=8\pi\overline{nT}/H_\varphi^2$, obtained from the diamagnetic measurements, and β_{Jl}, computed from the laser scattering data for a 7-μsec discharge. In computing β_{Jl}, we took the $\bar{n}_e$ dependence of $T_e(0)$ shown in Fig. 6 and the $T_e(r)$ and $n_e(r)$ profiles for the 7-μsec discharge (Fig. 4); it was assumed here that in the measured range of variation of $\bar{n}_e$ the $T_e(r,t)$ and $n_e(r,t)$ profiles do not change. The assumption (made above) that $Z_{eff}\sim 1$ and the assumption that the $T_e(r,t)$ and $n_e(r,t)$ profiles remain the same lead to some overestimation of the quantity β_{Jl}, but do not affect the qualitative dependence of β_{Jl} on $\bar{n}_e$. The large discrepancy between β_{Jd} and β_{Jl} at low plasma-concentration values is connected, apparently, with the presence in the plasma of fast electrons whose longitudinal energy is converted into transverse energy on account of Coulomb scattering, or because of the instability of the beam of runaway electrons. The role of the runaway electrons in the determination of T_d and β_{Jd} is estimated in[12]. As the electron concentration increases, the discrepancy between β_{Jd} and β_{Jl} decreases, and there exists a region of operating conditions of the TM-3 where the transverse electron energy measured by Thomson scattering coincides within the experimental errors with the value obtained in the diamagnetic measurements.

It is interesting to compare the dependence of $T_e(0)$ on the magnitude of the current and the longitudinal magnetic field of the TM-3 installation with the experimental dependences obtained on other Tokamak installations.[2-5] Because of the strong interdependence of the density, current, and temperature of the plasma in the TM-3 installation, it is not possible to investigate a

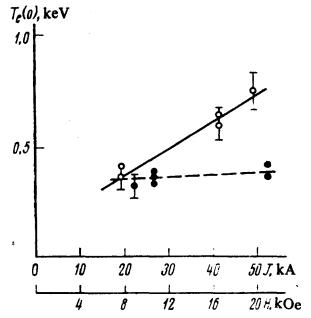

FIG. 7. Dependence of $T_e(0)$ on the magnitude of the discharge current (continuous curve) and on the longitudinal magnetic field (the dashed curve) for fixed $\bar{n}_e \approx 1.4\times10^{13}$ cm^{-3}.

large number of regimes with a fixed value of one of the parameters. Therefore, the graphs shown in Fig. 7 were constructed for a fixed value of $\bar{n}_e$ ($=1.4\times10^{13}$ cm^{-3}) in some close regimes. The electron temperature at the center of the column does not depend on the longitudinal magnetic field, which is characteristic of the majority of the Tokamak installations, and increases linearly with increasing current in the plasma. The dependence on current is not so strong as in the T-3A installation[2]; by its nature it is close to the data obtained on the ORMAK installation.[4]

The author considers it his pleasant duty to express his thanks to V. V. Alikaev, G. A. Bobrovskiĭ, K. A. Razumova, Yu. A. Sokolov, and D. A. Shcheglov for constant interest and help in the work, as well as to the technical staff of the TM-3 installation for their help in the carrying out of the experiment.

[1]N. J. Peacock, D. C. Robinson, M. J. Forrest, P. D. Wilcock, and V. V. Sannikov, Nature **224**, 448 (1969).
[2]M. J. Forrest, N. J. Peacock, D. C. Robinson, V. V. Sannikov, and P. D. Wilcock, CLM-R107, 1970.
[3]A. M. Anashin, E. P. Gorbunov, D. P. Ivanov, S. E. Lysenko, N. J. Peacock, D. C. Robinson, V. V. Sannikov, and V. S. Strelkov, Zh. Eksp. Teor. Fiz. **60**, 2092 (1971) [Sov. Phys. JETP **33**, 1127 (1971)].
[4]D. L. Dimock, H. P. Eubank, L. C. Johnson, and E. B. Meservey, Nucl. Fusion **13**, 271 (1973).
[5]M. Mukarami, W. Wing, and P. Edmonds, Nucl. Fusion **14**, 779 (1974).
[6]H. P. Furth, Nucl. Fusion **15**, 487 (1975).
[7]A. B. Berlizov, G. E. Notkin, and V. V. Sannikov, Preprint IAÉ-2583, 1975.
[8]A. L. Mikaélyan, M. L. Ter-Mikaélyan, and Yu. G. Turkov, Opticheskie generatory na tverdom tele (Solid-State Lasers), Sovetskoe Radio, 1967, p. 48.
[9]J. Sheffield, Plasma Phys. **14**, 783 (1972).
[10]V. A. Zhuravlev and G. D. Petrov, Opt. Spektrosk. **33**, 36 (1972) [Opt. Spectrosc. (USSR) **33**, 19 (1972)].
[11]L. A. Artsimovich, A. V. Glukhov, and M. P. Petrov, Pis'ma Zh. Eksp. Teor. Fiz. **11**, 449 (1970) [JETP Lett. **11**, 304 (1970)].
[12]V. V. Sannikov and Yu. A. Sokolov, Fiz. Plazmy **2**, 204 (1976) [Sov. J. Plasma Phys. **2**, 112 (1967)].
[13]E. P. Gorbunov, S. V. Mirnov, and V. S. Strelkov, Preprint IAÉ-1681 (1968).

Translated by A. K. Agyei

Spatially non-uniform singular weak turbulence spectra

V. S. L'vov and A. M. Rubenchik

Institute of Automation and Electrometry, Siberian Division USSR Academy of Sciences
(Submitted February 27, 1976; resubmitted July 23, 1976)
Zh. Eksp. Teor. Fiz **72**, 127–140 (January 1977)

We consider spatially non-uniform collective oscillations of singular weak turbulence spectra. We study the modulational instability of Langmuir turbulence spectra leading to collapse. We find its maximum growth rate and study the non-linear stage. We formulate equations describing the non-linear stage of the parametric instability in a non-uniform medium. We study the collective oscillations of a system of parametrically excited waves. We consider also the analogous problem of the effect of sample boundaries on the distribution of the oscillations. We estimate the dimensions for which a transition to the spatially non-uniform solution occurs.

PACS numbers: 47.25.−c

§1. INTRODUCTION

The traditional way to describe weak wave turbulence in a spatially non-uniform situation is to use the kinetic equation

$$\frac{\partial n_k}{\partial t}+\frac{\partial \omega_k}{\partial \mathbf{k}}\frac{\partial n_k}{\partial \mathbf{r}}-\frac{\partial \omega_k}{\partial \mathbf{r}}\frac{\partial n_k}{\partial \mathbf{k}}=\mathrm{St}\{n_k\}. \qquad (1.1)$$

It describes waves as weakly interacting quasi-particles; its right-hand side is caused by the "collisions of quasi-particles" with a large change in their momentum, while the left-hand side is the total derivative dn_k/dt. The spatial dependence can be caused by the inhomogeneity of the medium and may occur spontaneously due to the non-linear interaction of the oscillations.

For applications of Eq. (1.1) it is necessary to satisfy the adiabaticity condition $kL \gg 1$, which presupposes that the inhomogeneity dimension L is large compared with the wavelength k^{-1}. Moreover, in order that the